Characterization of the novel *Trypanosoma brucei* inosine 5′-monophosphate dehydrogenase

TOMOAKI BESSHO[1], SHOKO MORII[1], TOSHIHIDE KUSUMOTO[1], TAKAHIRO SHINOHARA[1], MASANORI NODA[2], SUSUMU UCHIYAMA[2], SATOSHI SHUTO[3], SHIGENORI NISHIMURA[1], APPOLINAIRE DJIKENG[4,5], MICHAEL DUSZENKO[6], SAMUEL K. MARTIN[7]†, TAKASHI INUI[1]* *and* KILUNGA B. KUBATA[8]*

[1] *Laboratory of Biological Macromolecules, Graduate School of Life and Environmental Sciences, Osaka Prefecture University, 1-1 Gakuen-cho, Naka-ku, Sakai, Osaka 599-8531, Japan*
[2] *Department of Biotechnology, Graduate School of Engineering, Osaka University, 2-1 Yamadaoka, Suita, Osaka 565-0871, Japan*
[3] *Laboratory of Organic Chemistry for Drug Development, Faculty of Pharmaceutical Sciences, Hokkaido University, Nishi 6, Kita 12, Kita-ku, Sapporo 060-0812, Japan*
[4] *Biosciences eastern and central Africa (BecA) Hub at the International Livestock Research Institute (ILRI), P.O. Box 30709, Nairobi, Kenya*
[5] *The J Craig Venter Institute (JCVI), Rockville, MD 20876, USA*
[6] *Interfaculty Institute of Biochemistry, University of Tübingen, Hoppe-Seyler-Straße 4, 72076 Tübingen, Germany*
[7] *Retired from United States Army Medical Research Unit-Kenya, Unit 64109, APO AE 09831-64109*
[8] *AU/NEPAD Agency Regional Office for Eastern and Central Africa, P.O. BOX 13601-00800, Nairobi, Kenya*

(*Received 5 September 2012; revised 8 November 2012; accepted 9 November 2012; first published online 1 February 2013*)

SUMMARY

There is an alarming rate of human African trypanosomiasis recrudescence in many parts of sub-Saharan Africa. Yet, the disease has no successful chemotherapy. *Trypanosoma* lacks the enzymatic machinery for the *de novo* synthesis of purine nucleotides, and is critically dependent on salvage mechanisms. Inosine 5′-monophosphate dehydrogenase (IMPDH) is responsible for the rate-limiting step in guanine nucleotide metabolism. Here, we characterize recombinant *Trypanosoma brucei* IMPDH (TbIMPDH) to investigate the enzymatic differences between TbIMPDH and host IMPDH. Size-exclusion chromatography and analytical ultracentrifugation sedimentation velocity experiments reveal that TbIMPDH forms a heptamer, different from type 1 and 2 mammalian tetrameric IMPDHs. Kinetic analysis reveals calculated K_m values of 30 and 1300 μM for IMP and NAD, respectively. The obtained K_m value of TbIMPDH for NAD is approximately 20–200-fold higher than that of mammalian enzymes and indicative of a different NAD binding mode between trypanosomal and mammalian IMPDHs. Inhibition studies show K_i values of 3·2 μM, 21 nM and 3·3 nM for ribavirin 5′-monophosphate, mycophenolic acid and mizoribine 5′-monophosphate, respectively. Our results show that TbIMPDH is different from its mammalian counterpart and thus may be a good target for further studies on anti-trypanosomal drugs.

Key words: trypanosome, enzyme kinetics, enzyme inhibitor, nucleoside nucleotide analogues, drug design.

INTRODUCTION

Human African trypanosomiasis (HAT) is caused by the infection of *Trypanosoma brucei* (*T. brucei*) *gambiense* and *T. brucei rhodesiense*, which are transmitted to the human host by bites of tsetse flies. HAT threatens more than 70 million people, who live in endemic areas with 50 000 and 70 000 new infections per year (Welburn and Odiit, 2002; World Health Organization, 2007) and is fatal if untreated. It is endemic mainly in sub-Saharan Africa, where the disease shows the highest prevalence rate, 60% in some villages in the Democratic Republic of the Congo (Smith *et al*. 1998; Welburn and Odiit, 2002). HAT has been considered an essentially rural disease until recently. However, it has become a significant public health threat in large cities such as Brazzaville in the Congo Republic, Kinshasa in the Democratic Republic of the Congo and Conakry in the Guinea Republic (Smith *et al*. 1998; Bilengue *et al*. 2001). Therapy for HAT relies still upon drugs, i.e. pentamidine, suramin, melarsoprol (trivalent arsenical) and eflornithine (difluoromethyl-ornithine) that

* Corresponding authors: Dr Takashi Inui, Laboratory of Biological Macromolecules, Graduate School of Life and Environmental Sciences, Osaka Prefecture University, 1-1 Gakuen-cho, Naka-ku, Sakai, Osaka 599-8531, Japan. Tel: +81-72-254-9473, Fax: +81-72-254-9921. E-mail: inuit@bioinfo.osakafu-u.ac.jp
Fr Kilunga B. Kubata, AU/NEPAD Agency Regional Office for Eastern and Central Africa, P.O. BOX 13601-00800, Nairobi, Kenya. Tel: +254 733 665210/ +254 737 966687. E-mail: bkkubata@nepadst.org / brunokubata@yahoo.com
† Present address: Esingila Health & Wellness Consultants, Inc. 2916 Cabin Creek Drive, Burtonsville, MD 20866, USA.

doi:10.1017/S0031182012002090

were first introduced over 50 years ago (Gutteridge, 1985; Doua and Yapo, 1993; Barrett *et al*. 2007). Pentamidine and suramin are used for the treatment of the early haemolymphatic stages of HAT, whereas melarsoprol is used for treatment of the late central nervous system stages of the disease. However, the latter requires parenteral administration and causes a reactive encephalopathy in up to 10% of treated patients, with a mortality rate of up to 5%. Recently, 25–30% of patients in Central Africa with late-stage HAT have not responded to melarsoprol due most likely to the emergence of drug-resistant strains of the parasite (Ross and Sutherland, 1997). Eflornithine is effective for late-stage infections caused by *T. brucei gambiense* (Burri and Brun, 2003), including many cases of arsenical resistance but ineffective against infections caused by *T. brucei rhodesiense* (Pepin and Milord, 1994; Iten *et al*. 1997; Barrett *et al*. 2007). However, it requires the parenteral administration of large doses and also shows some toxic side-effects. Currently, there are no other drug candidates in the pharmaceutical pipelines for HAT. This uncertainty for a successful chemotherapy against HAT and the lack of immediate vaccine candidates against *T. brucei* infections add impetus to explore the basic metabolic pathways of trypanosomes in order to identify novel drug targets; the rational approach for a new drug design being the identification and exploration of targets which are unique and/or different from those of the host in the basic biochemistry of the parasites. One such biochemical pathway is the biosynthesis of guanine nucleotide that is a rich source of therapeutic targets. However, since many of the major metabolic pathways in eukaryotic parasites are similar or identical to those in their vertebrate host, it is generally difficult to devise selective therapies against these parasites. One metabolic pathway that is conspicuously different between parasites and humans is that for the production of purine nucleotides. Whereas mammalian cells synthesize purine nucleotides *de novo, T. brucei* is auxotrophic for purines and critically dependent on salvage mechanisms to acquire purine nucleotides from the extracellular environment.

Guanine nucleotides are involved in many cellular functions including transmembrane and intracellular signalling (Parandoosh *et al*. 1989, 1990; Kharbanda *et al*. 1990; Mandanas *et al*. 1993; Manzoli *et al*. 1995), DNA replication, and RNA and protein synthesis (Jayaram *et al*. 1982). *De novo*, guanosine 5′-monophosphate (GMP) is synthesized from inosine 5′-monophosphate (IMP). In this pathway, IMPDH (EC 1.1.1.205) catalyses the NAD-dependent oxidation reaction of IMP that is converted into xanthosine 5′-monophosphate (XMP) as shown in BOX 1 of Fig. 1. Subsequently, XMP is converted into GMP (BOX 2 of Fig. 1) by GMP synthase (EC 6.3.4.1 or 6.3.5.2). IMPDH is the rate-limiting enzyme in guanine nucleotide biosynthesis

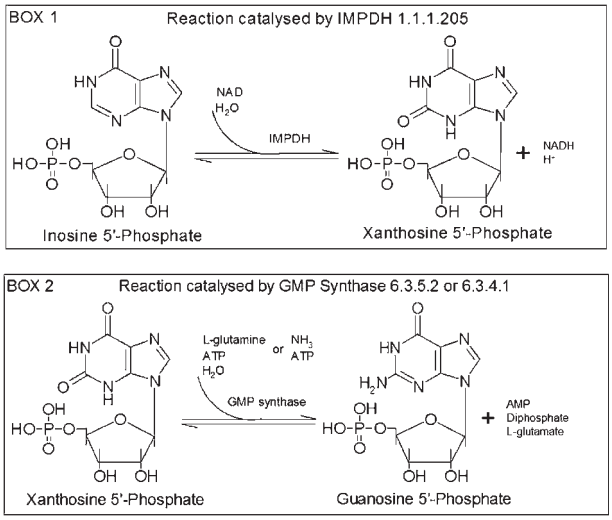

Fig. 1. Guanosine 5′-monophosphate biosynthetic pathway.

and also a key enzyme in the regulation of cell proliferation and differentiation (Wang and Hedstrom, 1997; Markham *et al*. 1999; Digits and Hedstrom, 1999a). It has been the target of antiviral (Witkowski *et al*. 1972; Patterson and Fernandez-Larsson, 1990; Poynard *et al*. 1998; Crotty *et al*. 2000; Maag *et al*. 2001), antimicrobial, anti-cancer (Weber *et al*. 1996) and immunosuppressive (Wu, 1994) therapies. IMPDHs have been found in almost every organism. In human, 2 isoenzymes of IMPDH have been identified, i.e. IMPDH type 1 which is constitutively expressed and IMPDH type 2 whose expression is up-regulated with peak enzyme activity occurring during the S phase of the cell cycle (Szekeres *et al*. 1992). All IMPDHs described so far are tetrameric proteins (Table S1, online version only). Literature and database search of trypanosome genome for the presence of IMPDH gene led to find a *T. brucei gambiense* nucleotide sequence of IMPDH gene (NCBI data bank ID: XM_822988) amplified due to an increase in chromosome copy number following treatment of this parasite with an excess amount of mycophenolic acid (MPA), an inhibitor of IMPDH (Wilson *et al*. 1994).

In this paper, we cloned and heterologously expressed TbIMPDH in *Escherichia coli* (*E. coli*), and showed that TbIMPDH is a unique large heptameric protein different from type 1 and 2 mammalian tetrameric IMPDHs. Kinetic analysis of TbIMPDH confirmed that the trypanosomal enzyme is indeed different from their mammalian counterparts, indicating that it is a good target for further studies on anti-trypanosomal drugs.

MATERIALS AND METHODS

Materials

IMP, NAD and MPA were purchased from Sigma Chemical Co. (St Louis, MO, USA). Ribavirin

https://doi.org/10.1017/S0031182012002090 Published online by Cambridge University Press

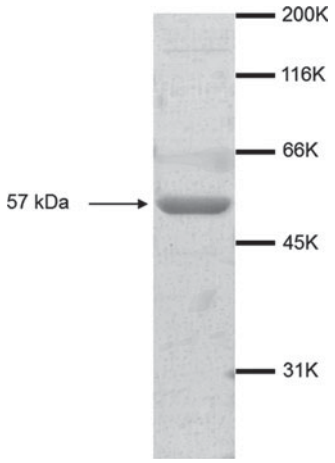

Fig. 2. SDS-PAGE analysis of purified TbIMPDH. The purified TbIMPDH of 3 μg was analysed by SDS-PAGE. The migration positions of the molecular mass standards are indicated on the right side. Marker proteins myosin (200 kDa), β-galactosidase (116 kDa), albumin (66 kDa), ovalbumin (45 kDa) and carbonic anhydrase (31 kDa) were used. Bands were visualized by staining the gel with Coomassie brilliant blue.

5′-monophosphate (RMP) was purchased from Toronto Research Chemicals Inc. (North York, Canada). Mizoribine 5′-monophosphate (MZP) was synthesized as previously described (Shuto *et al*. 2000). PIC-A was purchased from Waters Co. (Milford, MA, USA) and diluted according to the manufacturer's manual to give a 5 mM tetrabutylammonium phosphate solution of pH 7·0. All other chemicals were of analytical grade.

Expression and purification of TbIMPDH

The full-length TbIMPDH gene (NCBI data bank ID: XM_822988) was PCR amplified from *T. brucei* Tb427 strain genomic DNA and ligated into the *Eco*RI-*Sal*I sites of the expression vector pGEX-6P-1 plasmid (GE Healthcare BioScience, NJ, USA). Inserts of all clones were sequenced to reconfirm their sequences at the J Craig Venter Institute (JCVI, Rockville, MD, USA). *E. coli* BL21 (DE3) was transformed with the plasmid (TOYOBO, Tokyo, Japan) and the recombinant TbIMPDH was expressed as a GST fusion protein. The fusion protein was bound to glutathione-Sepharose 4B (GE Healthcare BioScience) and incubated with PreScission protease (GE Healthcare BioScience) to release TbIMPDH. The recombinant protein was further purified with a DEAE-TOYOPEARL anion exchange column (TOSOH, Tokyo, Japan). Protein purity was analysed by SDS-PAGE.

Size-exclusion chromatography

Size-exclusion chromatography was performed using the ÄKTA purifier HPLC apparatus equipped with a HiLoad 16/60 Superdex 200 pg gel-filtration column (GE Healthcare BioScience). The column was equilibrated and eluted with 50 mM Tris/Cl (pH 8·0) containing 150 mM KCl at a flow rate of 0·5 ml min^{-1}. The column was calibrated with a mixture of thyroglobulin, ferritin, human IgG, human transferrin and ovalbumin (molecular masses are 669, 440, 150, 81 and 43 kDa, respectively). The protein elution was monitored by UV absorption at 280 nm.

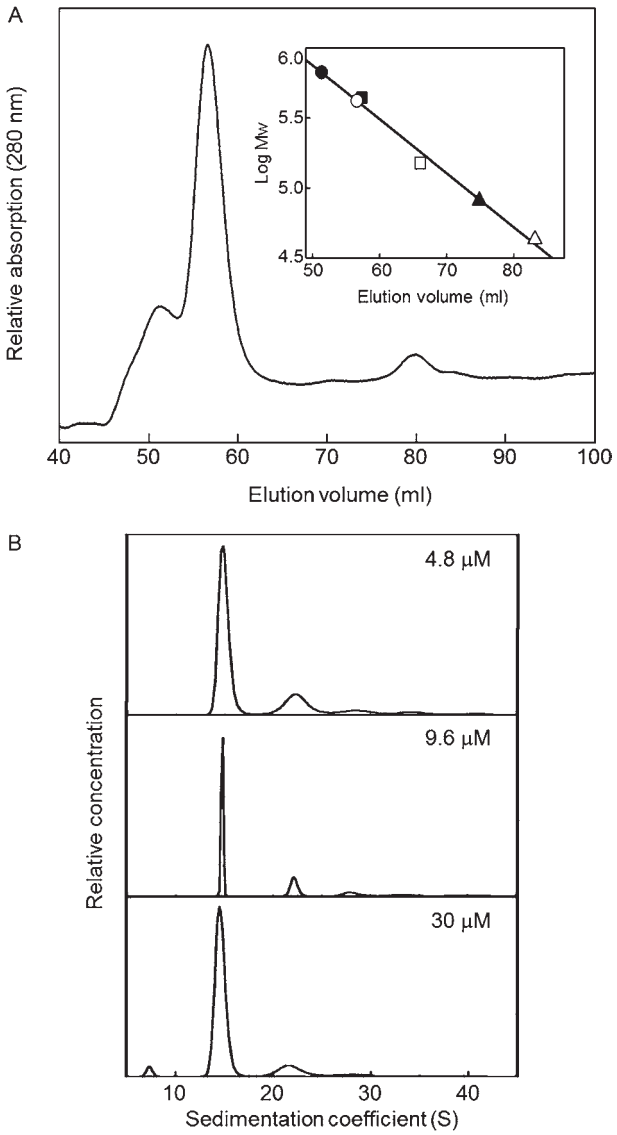

Fig. 3. Subunit structure of TbIMPDH. (A) Size-exclusion chromatography analysis of purified TbIMPDH. TbIMPDH was loaded onto a HiLoad 16/60 Superdex 200 pg gel-filtration column and eluted at the elution volume of 56·6 mL. Inset shows the calibration curve of the HiLoad 16/60 Superdex 200 pg gel filtration. Molecular mass standards: thyroglobulin (filled circle), ferritin (filled square), human IgG (open square), human transferrin (filled triangle) and ovalbumin (open triangle) were used. (B) Distribution states of TbIMPDH analysed by AUC-SV. Results of $C(s)$ analysis at different TbIMPDH concentrations are shown. The sedimentation coefficient was converted into $s_{20,w}$.

https://doi.org/10.1017/S0031182012002090 Published online by Cambridge University Press

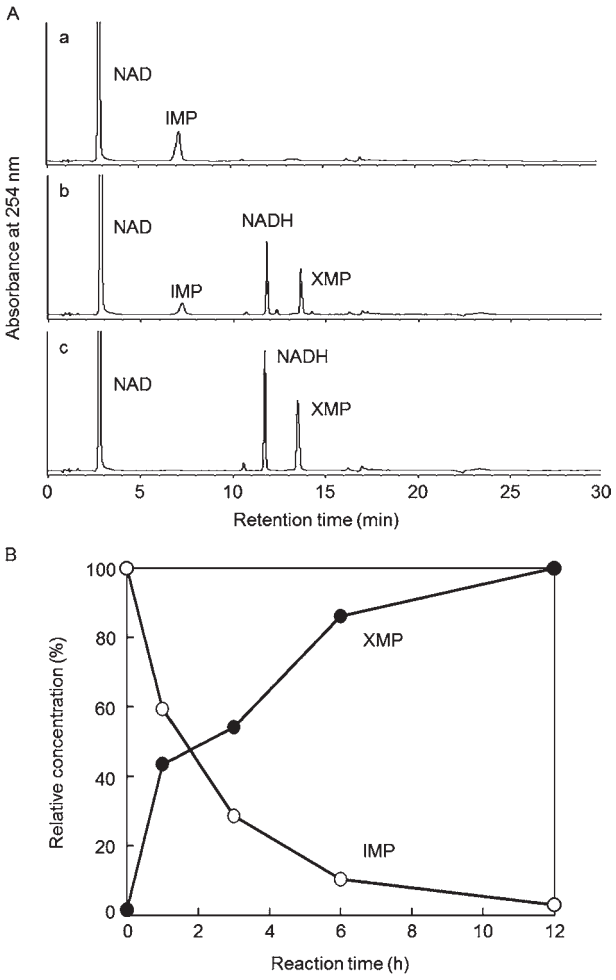

Fig. 4. Identification of TbIMPDH products. TbIMPDH (150 nM) was added to a solution containing 250 μM IMP and 1 mM NAD. (A) After incubation for 0 (a), 3 (b) and 25 (c) h at 25 °C, the reaction mixtures were separated by HPLC with a reversed-phase column at 35 °C. The mobile phase consisted of acetonitrile containing 0·1% trifluoroacetic acid (solvent A) and water containing 5 mM PIC-A reagent (solvent B). The gradient programmer was used according to the following procedure: 0–5 min hold on 5% A, 5–15 min linearly increase A from 5% to 50%, 15–20 min hold on 95% A, 20–30 min hold on 5% A with a flow-rate of 300 μL min^{-1}. The elution was monitored at 254 nm. (B) Consumption of IMP and formation of XMP by TbIMPDH.

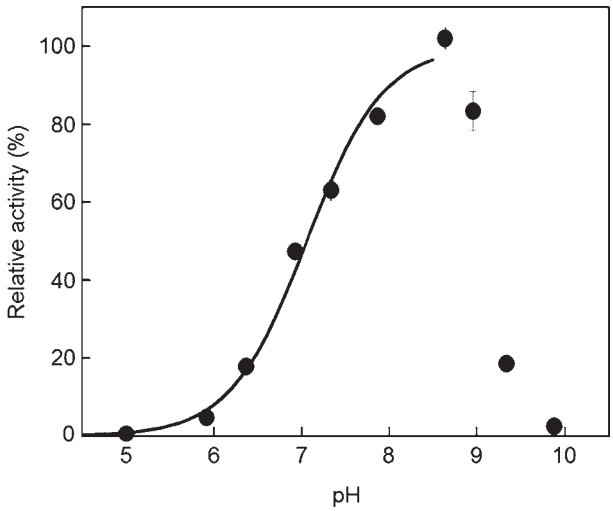

Fig. 5. pH dependence of activity for TbIMPDH. Relative activity is plotted *vs* pH. The plots are normalized by setting the value at pH 8·5 to 100%. Measurements were carried out at 25 °C in the buffers described in the experimental section. The experiment was conducted 3 times at each pH. The values are expressed as the mean ± S.E.

AUC-SV experiment

AUC-SV experiments were performed in 50 mM potassium phosphate (pH 7·4) containing 150 mM KCl using a ProteomeLab XL-I Analytical Ultracentrifuge (Beckman-Coulter, Fullerton, CA, USA). Samples of TbIMPDH of different concentrations (4·8, 9·6 and 30 μM) were measured. Centrifugations were carried out at 29, 46 and 66×10^3 ***g*** at a temperature of 20 °C using a 12 mm filled-epon double sector centrepiece and four-hole An60 Ti analytical rotor equilibrated to 20 °C. Sedimentation was monitored with absorbance detection optics at appropriate wavelengths (226, 227 and 230 nm) according to the concentration of the solution and within the solution absorbance of between 0·8 and 1·3. The radial increment was 0·003 cm and at least 150 scans were collected between 5·9 and 7·25 cm from the centre of rotation axis. All SV raw data were analysed using a continuous $C(s)$ distribution model with the SEDFIT11·71 program software (Schuck, 2000). The position of the meniscus and the frictional ratio (f/f_0) were set to vary as fitted parameters. A resolution of 300 increments between 0·1 and 50 S was entered and maximum entropy regularization was used (p = 0·68).

HPLC analysis of TbIMPDH products

The reaction mixture contained 50 mM Tris/Cl (pH 8·0), 100 mM KCl, 3 mM EDTA, 250 μM IMP, 1 mM NAD and 150 nM enzyme. After filtering 500 μL of the reaction mixture using VIVASPIN 500 (Sartorius K.K, Tokyo, Japan), 10 μL of the filtrate were injected for HPLC analysis. HPLC analysis was carried out using an Agilent 1100 series HPLC system (Agilent Technologies, Waldbronn, Germany) equipped with a quaternary pump, an online degasser, a column oven, and a diode-array detector. A Cosmosil 5C18 MS-II column (2·0 mm × 150 mm, 5 μm, Nacalai Tesque, Kyoto, Japan) was used for separation at a column temperature of 35 °C. The mobile phase consisted of acetonitrile containing 0·1% trifluoroacetic acid (solvent A) and water containing 5 mM PIC-A reagent (solvent B). The gradient programmer was used according to the following procedure: 0–5 min hold on 5% A, 5–15 min linearly increase A from 5 to 50%, 15–20 min hold on 95% A, 20–30 min

https://doi.org/10.1017/S0031182012002090 Published online by Cambridge University Press

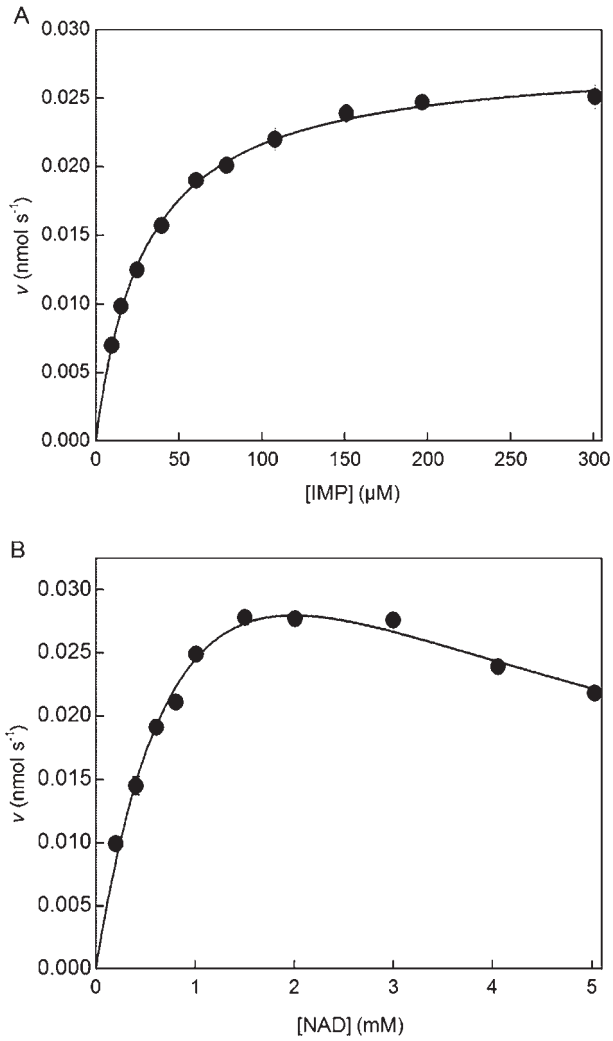

Fig. 6. Steady-state kinetics of TbIMPDH. (A) The plot of initial velocity *vs* the concentration of IMP at a fixed concentration of NAD (1·5 mM). Data were fitted to a Michaelis–Menten equation. (B) The plot of initial velocity *vs* the concentration of NAD at a fixed concentration of IMP (300 μM). Data were fitted to Equation 1, which describes uncompetitive substrate inhibition. The experiment was conducted 3 times at each concentration of substrate. The values are expressed as the mean ± S.E.

hold on 5% A with a flow-rate of 300 μL min^{-1}. The UV detection wavelength was set at 254 nm.

Dependence of TbIMPDH activity on pH

Measurements of TbIMPDH activity at different pH were performed in the following buffers: sodium acetate (pH 4·0–6·0), sodium phosphate (pH 6·0–7·5), Tris/Cl (pH 7·5–9·0), CHES (pH 9·0) and carbonate (pH 10·0). The ionic strengths of these buffers were adjusted to 0·25 by adding NaCl. Reactions were initiated by adding IMP in a reaction mixture of 500 μM IMP, 1 mM NAD and 150 nM enzyme and incubating at 25 °C for 10–40 min.

Enzyme kinetics

Standard IMPDH buffer contained 50 mM Tris/Cl (pH 8·0), 100 mM KCl, 3 mM EDTA and 1 mM DTT. The concentrations of IMP and NAD were varied to determine kinetic parameters. Reactions were initiated by the addition of IMP after the pre-incubation of the reaction mixture at 25 °C for 5 min and the activity was assayed in the presence of 200 nM enzyme at 25 °C for 10–40 min. NADH production was monitored at 340 nm (ε_{340} = 6220 M^{-1} cm^{-1}) and 25 °C using a UV-1600PC spectrophotometer (Shimadzu, Kyoto, Japan). Since substrate inhibition was observed, the initial velocity data were fitted into the Michaelis–Menten equation and uncompetitive substrate inhibition Equation 1 using Origin 6·0 software (Microcal, Northampton, MA, USA).

$$v = V_m/(1+K_m/[S] + [S]/K_{ii}) \quad (1)$$

where: K_m and K_{ii} represent the Michaelis constant and substrate inhibition constant, respectively.

Inhibitor kinetics

For the K_i value for RMP, experiments were carried out in the presence of constant concentrations of NAD (1·5 mM) but varied concentrations of RMP and IMP. For the K_i value for MPA, reactions were performed in the presence of 300 μM IMP and varied concentrations of MPA and NAD. The K_i value for MZP was measured in reaction mixtures containing 160 μM IMP and 1·5 mM NAD, and varied MZP concentrations. All the reaction mixtures contained 200 nM enzyme and were incubated at 25 °C for 5 min.

Data analysis for inhibition studies

Initial rate data were fitted to the competitive inhibition Equation 2, uncompetitive inhibition Equation 3 and the slow tight-binding competitive inhibition Equations 4 and 5 (Kerr and Hedstrom, 1997) using Origin 6·0 software. The best fits were determined by the relative fit error.

$$v = V_m[S]/(K_m(1 + [I]/K_i) + [S]) \quad (2)$$

$$v = V_m[S]/(K_m + [S](1 + [I]/K_i)) \quad (3)$$

$$[NADH] = [E_t]k_2k_{cat}t/b + [E_t][I]k_1'k_{cat}(1 - e^{-bt})/b^2 \quad (4)$$

$$b = [I]k_1' + k_2 \quad (5)$$

$[E_t]$ is the total concentration of enzyme, and [I] and K_i are the total concentration of inhibitor and the inhibition constant, respectively. k_1' is the observed association rate constant for inhibitor binding to enzyme, k_2 is the dissociation rate of the inhibitor enzyme complex, and k_{cat} is the observed catalytic

https://doi.org/10.1017/S0031182012002090 Published online by Cambridge University Press

Table 1. Comparison of the kinetic parameters of IMPDH

	k_{cat} (s^{-1})	$K_{m\ (IMP)}$ (μM)	$K_{m\ (NAD)}$ (μM)	$K_{ii\ (NAD)}$ (mM)	Reference
T. brucei	0·28	30 ± 1·2	1300 ± 300	3·0 ± 0·8	
*L. donovani**	0·7	33	390	–	(Dobie *et al*. 2007)
S. pyogenes	24	62	1180	ND	(Zhang *et al*. 1999)
C. parvum	3·3	29	150	2·9	(Umejiego *et al*. 2004)
T. foetus	1·9	1·7	150	6·8	(Digits & Hedstrom, 1999a)
Human type 1	1·2	17	70	2	(Mortimer & Hedstrom, 2005)
Human type 2	0·4	4	6	0·59	(Wang & Hedstrom, 1997)

* *L. donovani*, *Leishmania donovani*; assays were performed in 100 mM KCl, 50 mM Tris, pH 7·5, 2 mM DTT and 2 mM EDTA at 25 °C.
S. pyogenes, *Streptococcus pyogenes*; assay condition was not described (Zhang *et al*. 1999).
C. parvum, Cryptosporidium parvum; assays were performed in 100 mM KCl, 50 mM Tris, pH 8·0, 1 mM DTT and 3 mM EDTA at 25 °C.
T. foetus, Tritrichomonas foetus; assays were performed in 100 mM KCl, 50 mM Tris, pH 8·0, 1 mM DTT and 3 mM EDTA at 25 °C.
Human type 1; assays were performed in 100 mM KCl, 50 mM Tris, pH 8·0 and 1 mM DTT at 37 °C.
Human type 2; assays were performed in 100 mM KCl, 50 mM Tris, pH 8·0, 1 mM DTT and 2 mM EDTA at 25 °C.
-, Not detected.
ND, no data.

rate constant. The true association rate constant for inhibitor binding to the enzyme was obtained from Equation 6 and K_i was calculated with Equation 7:

$$k_1 = (K_m + [IMP])k_1^{'}/K_m \quad (6)$$

$$K_i = k_2/k_1 \quad (7)$$

RESULTS

Characterization of TbIMPDH subunit structure

We searched the literature and database of the trypanosome genome for the presence of IMPDH gene and found a *T. b. gambiense* nucleotide sequence of IMPDH gene (NCBI data bank ID: XM_822988) that had been amplified due to an increase in chromosome copy number following treatment of *T. b. gambiense* with an excess amount of MPA (Wilson *et al*. 1994); an inhibitor of IMPDH. We cloned and heterologously expressed this IMPDH gene. The purified recombinant TbIMPDH yielded a discrete single homogenous protein band on SDS-PAGE. The monomeric molecular mass of TbIMPDH was found to be 57 kDa (Fig. 2). Size-exclusion chromatography analysis revealed that the estimated molecular mass of the native TbIMPDH was approximately 420 kDa (Fig. 3A).

Since the quaternary structure of the trypanosome enzyme was unusually large, we investigated the assembly state of TbIMPDH using analytical ultracentrifugation and sedimentation velocity (AUC-SV), which provides the molecular mass of a protein or protein mixture in solution (Oda *et al*. 2009; Nishio *et al*. 2010) in order to exclude the possibility of protein aggregation. $C(s)$ sedimentation coefficient distributions at different concentrations (4·8, 9·6 and 30 μM) were similar (Fig. 3B), indicating the absence of concentration-dependent interactions. The majority (more than 90%) of TbIMPDH had species at the sedimentation value (s-value) of 14·5 S. The molecular mass of major species at 30 μM using this s-value and fitted shape factor (f/f_0) is 389 kDa. Although it should be noted that f/f_0 is provided as an averaged value in $C(s)$ analysis and does not correspond to the value for only major species. This molecular mass value of 389 kDa is closer to the molecular mass of 401 kDa calculated from the amino acid sequence, indicating that indeed TbIMPDH is a heptameric protein. We then estimated the molecular mass of species with different s-values by using a Monte Carlo genetic algorithm analysis in which individual s-values, f/f_0 values and populations for different species were obtained by numerical analysis. The estimated molecular mass of major species from Monte Carlo genetic algorithm analyses ranged from 379 to 397 kDa, consistent with a heptameric structure for TbIMPDH (Fig. S1, online version only). The hydrodynamic parameters of the heptamer (s-value of 15·5 S and f/f_0 of 1·2) correspond to an oblate molecule with dimensions of 16·4 nm × 4·9 nm assuming 30% hydration.

Identification of TbIMPDH enzymatic reaction products

In order to confirm that indeed the trypanosomal enzyme is an IMPDH that converts IMP into XMP, we carried out an HPLC analysis of the products resulting from the enzymatic reaction of TbIMPDH. Attempts to identify TbIMPDH-generated XMP revealed that the reaction product resulting from NAD-dependent oxidation reaction of IMP displayed an elution time corresponding to that of the

https://doi.org/10.1017/S0031182012002090 Published online by Cambridge University Press

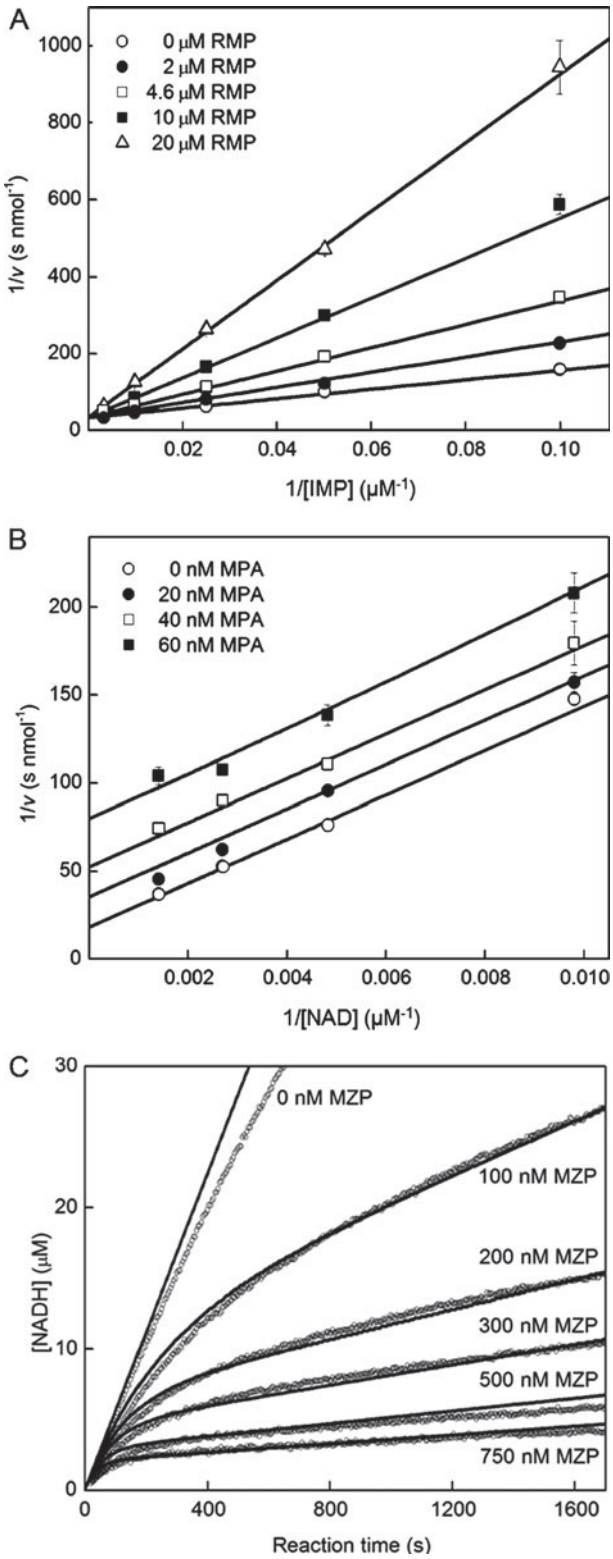

Fig. 7. Kinetic analysis of TbIMPDH inhibition. (A) Lineweaver–Burk double-reciprocal plots (1/*v vs* 1/[IMP]) for TbIMPDH activity are shown in the presence or absence of RMP. A mixture of 200 nM TbIMPDH, 1·5 mM NAD, 10–300 μM IMP and 0 (open circle), 2 (filled circle), 4·6 (open square), 10 (filled square) or 20 (open triangle) μM RMP was incubated for 5 min at 25 °C. The data were fitted to the equation describing competitive inhibition. (B) Lineweaver–Burk double-reciprocal plots (1/*v vs* 1/[NAD]) for TbIMPDH activity are shown in the presence or absence of MPA. A mixture of 200 nM TbIMPDH, 300 μM IMP, 100–700 μM NAD and 0 (open circle), 20 (filled circle), 40 (open square) or 60 (filled square) nM MPA was incubated for 5 min at 25 °C. The data were fitted to the equation describing uncompetitive inhibition. (C) Slow tight-binding competitive inhibition by MZP. A mixture of 200 nM TbIMPDH, 160 μM IMP 1·5 mM NAD and 0, 100, 200, 300, 500 or 750 nM MZP was incubated for 1800 s at 25 °C. The data were fitted to the equation describing slow tight-binding competitive inhibition.

authentic XMP (Fig. 4A). This figure shows also the chromatogram trace of the reaction mixture after incubation at 25 °C for 0 (a), 3 (b) and 25 (c) h. The elution times for NAD and IMP were 2·8 and 7·2 min, respectively, while those of XMP and NADH were 13·6 and 11·8 min, respectively, as compared with the elution times of authentic NAD, IMP, XMP and NADH. Moreover, the oxidation of IMP and biosynthesis of XMP were done in a time-dependent manner (Fig. 4B), confirming an enzyme-catalysed reaction of IMP conversion into XMP. Under our experimental conditions, no other enzymatic reaction products were identified. HPLC analysis results demonstrated that the TbIMPDH-generated product is indeed XMP and thus confirmed the fact that TbIMPDH catalyses specifically the oxidation of IMP into XMP.

Dependence of TbIMPDH activity on pH

As shown in Fig. 5, TbIMPDH exhibited the maximum enzymatic activity at around pH 8·5. However, this activity dropped down rapidly above this pH, suggesting probably that at pH > 8·5, the enzyme may well undergo an alkaline denaturation that would affect its activity. Additionally, to evaluate the alkaline denaturation of TbIMPDH at pH > 8·5, we performed circular dichroism (CD) measurements of TbIMPDH (Fig. S2, online version only). The secondary and ternary structures of protein can be determined by CD spectra in the far- and near-UV region, respectively. The far-UV CD spectra of TbIMPDH were almost identical shapes in the pH range from 7·87 to 9·88, indicating that there was no significant difference in secondary structure. On the other hand, the near-UV CD spectra of TbIMPDH were changed in a pH dependent-manner, suggesting that the ternary structure of aromatic residues are changed in the high pH range and thus TbIMPDH likely undergoes an alkaline denaturation.

Determination of TbIMPDH kinetics parameters

The study of kinetic parameters of TbIMPDH revealed that calculated K_m and k_{cat} values for IMP

https://doi.org/10.1017/S0031182012002090 Published online by Cambridge University Press

Table 2. Inhibition constants of IMPDH

	$K_{i\ (RMP)}$ (μM) (C)	$K_{i\ (MPA)}$ (nM) (UC)	$K_{i\ (MZP)}$ (nM) (SC)	Reference
T. brucei	3·2 ± 0·16	21 ± 3·5	3·3	
L. donovani	ND	25	ND	(Dobie *et al*. 2007)
S. pyogenes	6	> 10000	500	(Zhang *et al*. 1999)
C. parvum	ND	9300	11	(Umejiego *et al*. 2004)
T. foetus	0·065	9400	0·15	(Verham *et al*. 1987; Digits and Hedstrom, 1999b; Gan *et al*. 2003)
Human type 1	0·65	11	8·2	(Hager *et al*. 1995)
Human type 2	0·39	6	3·9	(Hager *et al*. 1995)

L. donovani, *Leishmania donovani*; assays were performed in 100 mM KCl, 50 mM Tris, pH 7·5, 2 mM DTT and 2 mM EDTA at 25 °C.
S. pyogenes, *Streptococcus pyogenes*; assay conditions were not described in Ref. (Zhang *et al*. 1999).
C. parvum, Cryptosporidium parvum; assays were performed in 100 mM KCl, 50 mM Tris, pH 8·0, 1 mM DTT and 3 mM EDTA at 25 °C.
T. foetus, Tritrichomonas foetus; assays for RMP were performed in 100 mM KCl, 50 mM Tris, pH 8·0 and 1 mM DTT at 25 °C, assays for MPA and MZP were performed in 100 mM KCl, 50 mM Tris, pH 8·0, 1 mM DTT and 3 mM EDTA at 25 °C.
Human type1; assay conditions were not described in Ref. (Hager *et al*. 1995).
Human type2; assay conditions were not described in Ref. (Hager *et al*. 1995).
C, competitive inhibition; UC, uncompetitive inhibition; SC, slow tight competitive inhibition; ND, no data.

were $30 \pm 1{\cdot}2\ \mu$M and $0{\cdot}28 \pm 0{\cdot}031\ s^{-1}$, respectively. Data of the initial velocity *versus* IMP concentration in the presence of 1·5 mM NAD were collected and fitted to the Michaelis-Menten equation (Fig. 6A). In contrast, the calculated apparent K_m and K_i values for NAD were $1300 \pm 290\ \mu$M and 3·00 ± 0·76 mM, respectively (Table 1) and data of the initial velocity *versus* concentration of NAD in the presence of 300 μM IMP were collected and fitted to the uncompetitive substrate inhibition equation (Equation 1, Fig. 6B).

Kinetics of TbIMPDH inhibitors

We assessed the inhibitory effects of the 3 chemicals on TbIMPDH. Figure 7 shows that RMP, MPA and MZP inhibited TbIMPDH activity in competitive (Fig. 7A), uncompetitive (Fig. 7B) and slow tight competitive inhibition (Fig. 7C) manners, respectively. Calculated K_i values for RMP, MPA and MZP were $3{\cdot}2 \pm 0{\cdot}16\ \mu$M, 21 ± 3·5 nM and 3·3 nM, respectively (Table 2).

DISCUSSION

Human African trypanosomiasis is re-emerging alarmingly in some parts of sub-Saharan Africa. However, the disease has no reliable chemotherapy. Existing drugs are limited in number, present side-effects and drawbacks, and in some cases drug-resistant strains of trypanosomes are emerging. In the past, we have been interested in the identification of new anti-trypanosomal drugs and characterized anti-trypanosomal activities of pro-anthocyanidin from *Kola acuminata* (Kubata *et al*. 2005) and artemisinin derivatives from *Artemisia annua* (Kubata *et al*. 2008). In *Trypanosoma*, conversion of IMP to XMP is the major pathway in GMP biosynthesis and thus IMPDH, which catalyses the conversion reaction, is essential for the survival of *Trypanosoma*. Therefore, we would expect that IMPDH inhibition causes cell death in *T. brucei*, and a TbIMPDH-specific inhibitor could be an effective anti-trypanosomal drug. So far, Wilson *et al*. (1994) reported identification of IMPDH mRNA and observation of IMPDH activity in the lysate of *T. brucei gambiense*. However, there is no other report related to the enzymatic properties of TbIMPDH. In the present study, we cloned and purified the recombinant TbIMPDH by using the *E. coli* expression system, and carried out the enzymatic characterization of TbIMPDH as a candidate of drug target. Thus, this is a first report for showing the enzymatic characterization of TbIMPDH. Further, we also determined the molecular mass of its denatured (subunit) and native forms. Experimental results showed that TbIMPDH is a very large heptameric protein with almost twice the size of all other tetrameric enzymes described so far. Although it is not yet clear why the trypanosomal enzyme appears as a heptamer, it is tempting to speculate that this structure provides TbIMPDH with additional functional features.

RMP, MPA and MZP are well-known inhibitors of IMPDH from various sources (Patterson and Fernandez-Larsson, 1990; Gan *et al*. 2002; Hong and Cameron, 2002; Gensburger *et al*.2009). Inhibition studies carried out showed that RMP, MPA and MZP were competitive, uncompetitive and slow tight-binding inhibitors, respectively of TbIMPDH as has been described previously. TbIMPDH K_i

https://doi.org/10.1017/S0031182012002090 Published online by Cambridge University Press

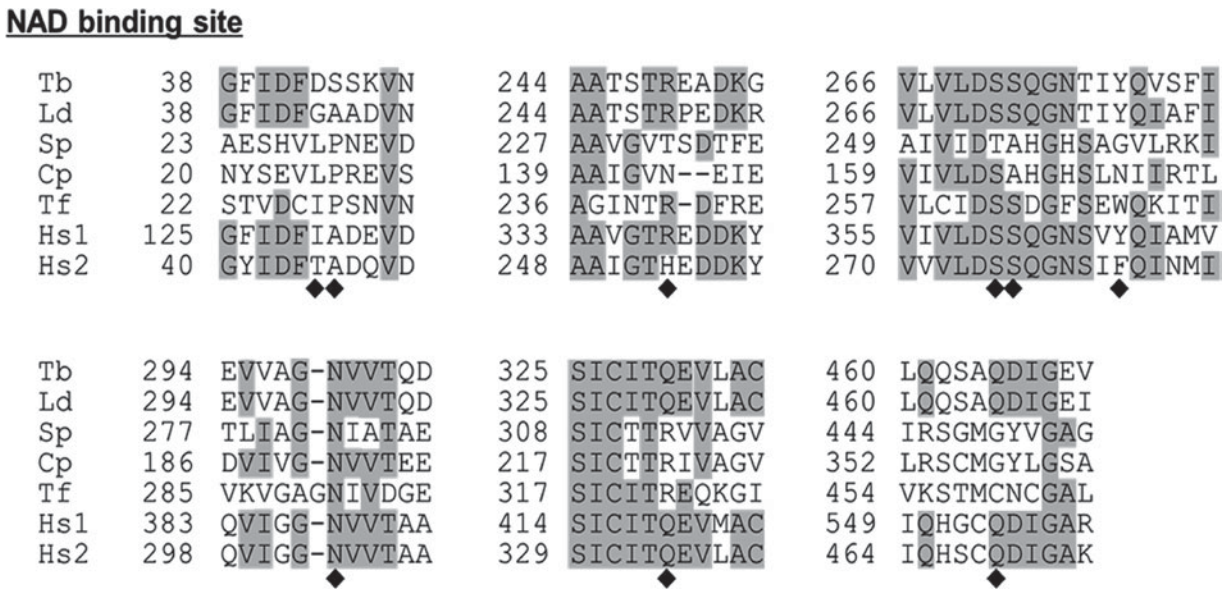

Fig. 8. Alignment of the amino acid sequences of the predicted NAD binding site. The primary structure of IMPDHs were aligned by using the CLUSTAL X2 program (Larkin *et al*. 2007). The NCBI ID for sequences used in the sequence alignment analysis were as follows: *Leishmania donovani* (AAA29253), *Streptococcus pyogenes* (YP_603464), *Cryptosporidium parvum* (AAL83208), *Tritrichomonas foetus* (AAB01581), human Type 1 (NP_000874) and human Type 2 (NP_000875). Identical amino acid residues in at least 4 of 7 sequences are indicated by a grey background. NAD binding residues in human IMPDH type 2 are indicated by ♦ symbols.

values of 3·2 ± 0·16 μM, 21 ± 3·5 nM and 3·3 nM, for RMP, MPA and MZP, respectively, are higher than those of mammalian type-enzymes, indicating that these chemicals are stronger inhibitors of mammalian rather than trypanosomal enzymes.

Interestingly, the K_m value of 1300 μM for NAD of TbIMPDH is about 20 to 200-fold higher than that of the mammalian counterpart (K_m value of 70 μM for NAD of human type 1 and K_m value of 6 μM for NAD of human type 2 IMPDHs), showing a difference in the mode and strength of binding of the cofactor NAD by both enzymes. *Streptococcus pyogenes* IMPDH (SpIMPDH) shows the higher K_m value for NAD than human IMPDH and the difference have been explained by the stacking interaction between enzyme and NAD. The K_m value of human IMPDH type 2 for NAD (K_m = 6 μM) is lower than that of human IMPDH type 1 for NAD (K_m = 70 μM), and the K_m value of human IMPDH type 1 for NAD is lower than that of SpIMPDH (K_m = 1180 μM) (Zhang *et al*. 1999). Colby *et al*. (1999) clarified the ternary complex between human IMPDH type 2 and the substrate and cofactor analogues, which are 6-Cl IMP and selenazole-4-carboxamide adenine dinucleotide (SAD). The crystal structure shows that the adenine ring of SAD stacks against the indole ring of His253 and aromatic ring of Phe282 in human IMPDH type 2. In human IMPDH type 1, these residues are replaced by Arg and Tyr, respectively, implying that these substitutions partially disrupt stacking interaction. In SpIMPDH, these residues are replaced by Thr and Gly, respectively, implying that these substitutions completely disrupt the stacking interaction (Fig. 8). The differences between the K_m values for NAD correlate with the substitutions of these residues. Thus, we speculated that TbIMPDH has the substitution of these residues such as Thr and Gly of SpIMPDH and the stacking interaction would be disrupted in TbIMPDH. However, these residues were replaced by Arg and Tyr in TbIMPDH, respectively, and similarly in human IMPDH type 1. The K_m values of TbIMPDH and human IMPDH type 1 for NAD were 1300 and 70 μM, respectively. Thus, the stacking interaction is probably unrelated to the high K_m value of TbIMPDH for NAD and other factors would influence the NAD binding of TbIMPDH.

On the other hand, the remarkable difference between the K_m values of trypanosomal and mammalian IMPDHs for NAD can most probably be explained by the NAD and NADH regenerating system of glycosome. Vertommen *et al*. (2008) reported that TbIMPDH is localized in the glycosome and actually TbIMPDH has a carboxyl-terminal Ser-Lys-Leu tripeptide, which is a glycosomal peroxisomal targeting signal. Glycosome possesses an NAD and NADH regenerating system in trypanosomatids (Michels *et al*. 2006) and the concentrations of coenzyme in the glycosome would be much higher than in the cytosol. It is considered that TbIMPDH needs a high concentration of NAD to exhibit the enzymatic activity at the high K_m value of TbIMPDH for NAD. As described above, TbIMPDH is localized in the glycosome, which possesses a large amount of NAD. Thus, TbIMPDH

https://doi.org/10.1017/S0031182012002090 Published online by Cambridge University Press

could exhibit the enzymatic activity in the glycosome, indicating that TbIMPDH adapts to its local environment. A high K_m value for NAD has also been reported for the parasitic enzyme *Cryptosporidium parvum* IMPDH (CpIMPDH) (Umejiego *et al*. 2004), and the NAD binding site of CpIMPDH was also identified as a potential drug target because of the difference between structure and properties of both the parasitic and mammalian enzymes. Actually, benzimidazole derivatives which target the NAD binding site showed a parasite-selective inhibition for CpIMPDH (Kirubakaran *et al*. 2012). Therefore, the difference in structure and properties between TbIMPDH and the mammalian enzymes makes TbIMPDH a good candidate for the development of more specific inhibitors targeting its NAD binding site. To achieve this, X-ray crystallographic studies of TbIMPDH and in complex with NAD are indispensable and we are currently working on this.

ACKNOWLEDGEMENTS

We thank Dr K. Fujimori, Ms M. Tabuchi and Ms C. Kimura for technical assistance and helpful discussions. This study was undertaken with the financial support of the Government of Canada provided through the Canadian International Development Agency to NEPAD. This study was also supported in part by the program Grants-in-Aid for Scientific Research of the Ministry of Education, Culture, Sports, Science and Technology of Japan and Osaka Prefecture (grant numbers 17300165, 21500428 and 21200076 (to T.I.)).

REFERENCES

World Health Organization (2007). African trypanosomiasis (sleeping sickness), Fact sheet No. 259. WHO, Geneva, Switzerland.

Barrett, M. P., Boykin, D. W., Brun, R. and Tidwell, R. R. (2007). Human African trypanosomiasis: pharmacological re-engagement with a neglected disease. *British Journal of Pharmacology* **152**, 1155–1171. doi: 10.1038/sj.bjp.0707354.

Bilengue, C. M., Meso, V. K., Louis, F. J. and Lucas, P. (2001). Human African trypanosomiasis in the urban milieu: the example of Kinshasa, Democratic Republic of the Congo, in 1998 and 1999. *Médecine tropicale: revue du Corps de santé colonial* **61**, 445–448.

Burri, C. and Brun, R. (2003). Eflornithine for the treatment of human African trypanosomiasis. *Parasitology Research* **90** (Suppl. 1), S49–S52. doi: 10.1007/s00436-002-0766-5.

Colby, T. D., Vanderveen, K., Strickler, M. D., Markham, G. D. and Goldstein, B. M. (1999). Crystal structure of human type II inosine monophosphate dehydrogenase: implications for ligand binding and drug design. *Proceedings of the National Academy of Sciences USA* **96**, 3531–3536. doi: 10.1073/pnas.96.7.3531.

Crotty, S., Maag, D., Arnold, J. J., Zhong, W., Lau, J. Y., Hong, Z., Andino, R. and Cameron, C. E. (2000). The broad-spectrum antiviral ribonucleoside ribavirin is an RNA virus mutagen. *Nature Medicine* **6**, 1375–1379. doi: 10.1038/82191.

Digits, J. A. and Hedstrom, L. (1999*a*). Kinetic mechanism of *Tritrichomonas foetus* inosine 5′-monophosphate dehydrogenase. *Biochemistry* **38**, 2295–2306. doi: 10.1021/bi982305k.

Digits, J. A. and Hedstrom, L. (1999*b*). Species-specific inhibition of inosine 5′-monophosphate dehydrogenase by mycophenolic acid. *Biochemistry* **38**, 15388–15397. doi: 10.1021/bi991558q.

Dobie, F., Berg, A., Boitz, J. M. and Jardim, A. (2007). Kinetic characterization of inosine monophosphate dehydrogenase of *Leishmania donovani*. *Molecular and Biochemical Parasitology* **152**, 11–21. doi: 10.1016/j.molbiopara.2006.11.007.

Doua, F. and Yapo, F. B. (1993). Human trypanosomiasis in the Ivory Coast: therapy and problems. *Acta Tropica* **54**, 163–168. doi: 10.1016/0001-706X(93)90090-X.

Gan, L., Petsko, G. A. and Hedstrom, L. (2002). Crystal structure of a ternary complex of *Tritrichomonas foetus* inosine 5′-monophosphate dehydrogenase: NAD+ orients the active site loop for catalysis. *Biochemistry* **41**, 13309–13317. doi: 10.1021/bi0203785.

Gan, L., Seyedsayamdost, M. R., Shuto, S., Matsuda, A., Petsko, G. A. and Hedstrom, L. (2003). The immunosuppressive agent mizoribine monophosphate forms a transition state analogue complex with inosine monophosphate dehydrogenase. *Biochemistry* **42**, 857–863. doi: 10.1021/bi0271401.

Gensburger, O., Picard, N. and Marquet, P. (2009). Effect of mycophenolate acyl-glucuronide on human recombinant type 2 inosine monophosphate dehydrogenase. *Clinical Chemistry* **55**, 986–993. doi: 10.1373/clinchem.2008.113936.

Gutteridge, W. E. (1985). Existing chemotherapy and its limitations. *British Medical Bulletin* **41**, 162–168.

Hager, P. W., Collart, F. R., Huberman, E. and Mitchell, B. S. (1995). Recombinant human inosine monophosphate dehydrogenase type I and type II proteins. Purification and characterization of inhibitor binding. *Biochemical Pharmacology* **49**, 1323–1329. doi: 0006-2952(95)00026-V [pii].

Hong, Z. and Cameron, C. E. (2002). Pleiotropic mechanisms of ribavirin antiviral activities. *Progress in Drug Research* **59**, 41–69.

Iten, M., Mett, H., Evans, A., Enyaru, J. C., Brun, R. and Kaminsky, R. (1997). Alterations in ornithine decarboxylase characteristics account for tolerance of *Trypanosoma brucei* rhodesiense to D,L-alpha-difluoromethylornithine. *Antimicrobial Agents and Chemotherapy* **41**(9), 1922–1925.

Jayaram, H. N., Dion, R. L., Glazer, R. I., Johns, D. G., Robins, R. K., Srivastava, P. C. and Cooney, D. A. (1982). Initial studies on the mechanism of action of a new oncolytic thiazole nucleoside, 2-beta-D-ribofuranosylthiazole-4-carboxamide (NSC 286193). *Biochemical Pharmacology* **31**, 2371–2380. doi: 10.1016/0006-2952(82)90532-9.

Kerr, K. M. and Hedstrom, L. (1997). The roles of conserved carboxylate residues in IMP dehydrogenase and identification of a transition state analog. *Biochemistry* **36**, 13365–13373. doi: 10.1021/bi9714161.

Kharbanda, S. M., Sherman, M. L. and Kufe, D. W. (1990). Effects of tiazofurin on guanine nucleotide binding regulatory proteins in HL-60 cells. *Blood* **75**, 583–588.

Kirubakaran, S., Gorla, S. K., Sharling, L., Zhang, M., Liu, X., Ray, S. S., Macpherson, I. S., Striepen, B., Hedstrom, L. and Cuny, G. D. (2012). Structure-activity relationship study of selective benzimidazole-based inhibitors of *Cryptosporidium parvum* IMPDH. *Bioorganic and Medicinal Chemistry Letters* **22**, 1985–1988. doi: 10.1016/j.bmcl.2012.01.029.

Kubata, B. K., Martin, S. K. and Milhous, W. K. (2008). Artemisinins in the clinical and veterinary management of kinetoplastid infections. In *International Patent* (ed. Organization, T. W. I. P.).

Kubata, B. K., Nagamune, K., Murakami, N., Merkel, P., Kabututu, Z., Martin, S. K., Kalulu, T. M., Huq, M., Yoshida, M., Ohnishi-Kameyama, M., Kinoshita, T., Duszenko, M. and Urade, Y. (2005). *Kola acuminata* proanthocyanidins: a class of anti-trypanosomal compounds effective against *Trypanosoma brucei*. *International Journal for Parasitology* **35**, 91–103. doi: 10.1016/j.ijpara.2004.10.019.

Larkin, M. A., Blackshields, G., Brown, N. P., Chenna, R., McGettigan, P. A., McWilliam, H., Valentin, F., Wallace, I. M., Wilm, A., Lopez, R., Thompson, J. D., Gibson, T. J. and Higgins, D. G. (2007). Clustal W and Clustal X version 2.0. *Bioinformatics* **23**, 2947–2948.

Maag, D., Castro, C., Hong, Z. and Cameron, C. E. (2001). Hepatitis C virus RNA-dependent RNA polymerase (NS5B) as a mediator of the antiviral activity of ribavirin. *Journal of Biological Chemistry* **276**, 46094–46098. doi: 10.1074/jbc.C100349200.

Mandanas, R. A., Leibowitz, D. S., Gharehbaghi, K., Tauchi, T., Burgess, G. S., Miyazawa, K., Jayaram, H. N. and Boswell, H. S. (1993). Role of p21 RAS in p210 bcr-abl transformation of murine myeloid cells. *Blood* **82**, 1838–1847.

Manzoli, L., Billi, A. M., Gilmour, R. S., Martelli, A. M., Matteucci, A., Rubbini, S., Weber, G. and Cocco, L. (1995). Phosphoinositide signaling in nuclei of Friend cells: tiazofurin down-regulates phospholipase C beta 1. *Cancer Research* **55**, 2978–2980.

Markham, G. D., Bock, C. L. and Schalk-Hihi, C. (1999). Acid-base catalysis in the chemical mechanism of inosine monophosphate dehydrogenase. *Biochemistry* **38**, 4433–4440. doi: 10.1021/bi9829579.

Michels, P. A., Bringaud, F., Herman, M. and Hannaert, V. (2006). Metabolic functions of glycosomes in trypanosomatids. *Biochimica Biophysica Acta* **1763**, 1463–1477. doi: 10.1016/j.bbamcr.2006.08.019.

Mortimer, S. E. and Hedstrom, L. (2005). Autosomal dominant retinitis pigmentosa mutations in inosine 5′-monophosphate dehydrogenase type I disrupt nucleic acid binding. *Biochemical Journal* **390**, 41–47. doi: 10.1042/BJ20042051.

Nishio, M., Kamiya, Y., Mizushima, T., Wakatsuki, S., Sasakawa, H., Yamamoto, K., Uchiyama, S., Noda, M., McKay, A. R., Fukui, K., Hauri, H. P. and Kato, K. (2010). Structural basis for the cooperative interplay between the two causative gene products of combined factor V and factor VIII deficiency. *Proceedings of the National Academy of Sciences, USA* **107**, 4034–4039.

Oda, M., Uchiyama, S., Noda, M., Nishi, Y., Koga, M., Mayanagi, K., Robinson, C. V., Fukui, K., Kobayashi, Y., Morikawa, K. and Azuma, T. (2009). Effects of antibody affinity and antigen valence on molecular forms of immune complexes. *Molecular Immunology* **47**, 357–364.

Parandoosh, Z., Robins, R. K., Belei, M. and Rubalcava, B. (1989). Tiazofurin and selenazofurin induce depression of cGMP and phosphatidylinositol pathway in L1210 leukemia cells. *Biochemical and Biophysical Research Communications* **164**, 869–874. doi: 10.1016/0006-291X(89)91539-8.

Parandoosh, Z., Rubalcava, B., Matsumoto, S. S., Jolley, W. B. and Robins, R. K. (1990). Changes in diacylglycerol and cyclic GMP during the differentiation of human myeloid leukemia K562 cells. *Life Sciences* **46**, 315–320.

Patterson, J. L. and Fernandez-Larsson, R. (1990). Molecular mechanisms of action of ribavirin. *Reviews of Infectious Diseases* **12**, 1139–1146.

Pepin, J. and Milord, F. (1994). The treatment of human African trypanosomiasis. *Advances in Parasitology* **33**, 1–47.

Poynard, T., Marcellin, P., Lee, S. S., Niederau, C., Minuk, G. S., Ideo, G., Bain, V., Heathcote, J., Zeuzem, S., Trepo, C. and Albrecht, J. (1998). Randomised trial of interferon alpha2b plus ribavirin for 48 weeks or for 24 weeks versus interferon alpha2b plus placebo for 48 weeks for treatment of chronic infection with hepatitis C virus. International Hepatitis Interventional Therapy Group (IHIT). *Lancet* **352**, 1426–1432. doi:10.1016/S0140-6736(98)07124-4.

Ross, C. A. and Sutherland, D. V. (1997). Drug resistance in trypanosomatids. In *Trypanosomiasis and Leishmaniasis: Biology and Control* (ed. Hide, G., Mottram, J. C., Coombs, G. H. and Holmes, P. H.), pp. 259–269. CAB International, Wallingford, UK.

Schuck, P. (2000). Size-distribution analysis of macromolecules by sedimentation velocity ultracentrifugation and lamm equation modeling. *Biophysical Journal* **78**, 1606–1619.

Shuto, S., Haramuishi, K., Fukuoka, M. and Matsuda, A. (2000). Synthesis of sugar-modified analogs of bredinin (mizoribine), a clinically useful immunosuppressant, by a novel photochemical imidazole ring-cleavage reaction as the key step 1. *Journal of the Chemical Society, Perkin Transactions 1* **21**, 3603–3609.

Smith, D. H., Pepin, J. and Stich, A. H. (1998). Human African trypanosomiasis: an emerging public health crisis. *British Medical Bulletin* **54**(2), 341–355.

Szekeres, T., Fritzer, M., Pillwein, K., Felzmann, T. and Chiba, P. (1992). Cell cycle dependent regulation of IMP dehydrogenase activity and effect of tiazofurin. *Life Sciences* **51**, 1309–1315.

Umejiego, N. N., Li, C., Riera, T., Hedstrom, L. and Striepen, B. (2004). *Cryptosporidium parvum* IMP dehydrogenase: identification of functional, structural, and dynamic properties that can be exploited for drug design. *Journal of Biological Chemistry* **279**, 40320–40327.

Verham, R., Meek, T. D., Hedstrom, L. and Wang, C. C. (1987). Purification, characterization, and kinetic analysis of inosine 5′-monophosphate dehydrogenase of *Tritrichomonas foetus*. *Molecular and Biochemical Parasitology* **24**, 1–12. doi:10.1016/0166-6851(87)90110-1.

Vertommen, D., Van Roy, J., Szikora, J. P., Rider, M. H., Michels, P. A. and Opperdoes, F. R. (2008). Differential expression of glycosomal and mitochondrial proteins in the two major life-cycle stages of *Trypanosoma brucei*. *Molecular and Biochemical Parasitology* **158**, 189–201. doi:S0166–6851(07)00344-1 [pii] 10.1016/j.molbiopara.2007.12.008.

Wang, W. and Hedstrom, L. (1997). Kinetic mechanism of human inosine 5′-monophosphate dehydrogenase type II: random addition of substrates and ordered release of products. *Biochemistry* **36**, 8479–8483. doi:10.1021/bi970226n.

Weber, G., Prajda, N., Abonyi, M., Look, K. Y. and Tricot, G. (1996). Tiazofurin: molecular and clinical action. *Anticancer Research* **16**, 3313–3322.

Welburn, S. C. and Odiit, M. (2002). Recent developments in human African trypanosomiasis. *Current Opinion in Infectious Diseases* **15**, 477–484.

Wilson, K., Berens, R. L., Sifri, C. D. and Ullman, B. (1994). Amplification of the inosinate dehydrogenase gene in *Trypanosoma brucei gambiense* due to an increase in chromosome copy number. *Journal of Biological Chemistry* **269**, 28979–28987.

Witkowski, J. T., Robins, R. K., Sidwell, R. W. and Simon, L. N. (1972). Design, synthesis, and broad spectrum antiviral activity of 1-β-d-ribofuranosyl-1,2,4-triazole-3-carboxamide and related nucleosides. *Journal of Medicinal Chemistry* **15**, 1150–1154.

Wu, J. C. (1994). Perspectives in drug discovery and design. In *Mycophenolate mofetil: Molecular Mechanisms of Action*, Vol. 2. pp. 185–204. Leiden, the Netherlands.

Zhang, R., Evans, G., Rotella, F. J., Westbrook, E. M., Beno, D., Huberman, E., Joachimiak, A. and Collart, F. R. (1999). Characteristics and crystal structure of bacterial inosine-5′-monophosphate dehydrogenase. *Biochemistry* **38**, 4691–4700. doi:10.1021/bi982858v.